INVESTIGATION OF POINT SPREAD FUNCTION FOR THE SPACEBORNE TELESCOPE OF THE ASTROPHYSICAL STATION "ASTRONB BASED ON THE DATA OF FIELD OBSERVATIONS OF THE SUN-ILLUMINATED MOON AND EARTH'S DISKS

A.A. Cheremisin, L.V. Granitskii, V.M. Myasnikov, N.V. Vetchinkin, and V.V. Slabko

Scientific Research Physical-Technical Institute at the Krasnoyarsk State University, Krasnoyarsk, Krasnoyarsk State Technical University, Krasnoyarsk, E.K. Fedorov Institute of Applied Geophysics, Moscow

Received October 17, 1997

Two-dimensional effective point spread function for the ultraviolet telescope mounted onboard the space astrophysical station "Astron" was reconstructed from the data of specially arranged observations of the moon and Earth's disks illuminated by the Sun by solving the relevant inverse problem. The range of the reconstructed function variation is about 10^{13}*. Several characteristic regions of the function variation have been revealed as caused by the telescope design peculiarities. The results are used for interpretation of the data of the upper Earth's atmosphere investigation.*

Detailed investigations of the instrumental functions that characterize the spatial response of optical systems allow one to solve some problems on the quality, spatial resolution, and the background level due to scattered radiation in the instrumentation. All this gives additional potentiality for reduction and interpretation of the remote sensing data.[1,2] The level of background due to spuriously scattered radiation is essential when making observations from space.[3] In particular, this factor is very important when observing the upper Earth's atmosphere under illumination of an instrument by such illumination sources as the illuminated Earth's disk and the Sun.

It is not problematic to measure the scattering on the order of 10^{-4} from some optical elements in the laboratory, whereas experimental difficulties become serious when measuring scattering light at the level of $10^{-6} - 10^{-7}$ (see Ref. 3). Investigation of that low scattering in the operating telescopic systems, especially large ones, is a very complicated task. Nevertheless, new possibilities for solving such a problem appear when investigating from space.

The space astrophysical station (AS) "Astron" was launched to a high-apogee orbit (200 thousand kilometers) on March 23, 1983. Since that time a series of experiments on investigating the upper atmosphere in the ultraviolet wavelength range with the AS ultraviolet telescope[4–6] has been carried out. The telescope is of the Ricci–Kretien system with the diameter of the primary mirror of 80 cm and the equivalent focal length of 786 mm, and it is conjugated with a Rowland-type spectrometer.

In this paper, we present the two-dimensional point spread function (PSF) for AS "Astron" telescope obtained as a result of solving the inverse problems based on the data of observations of the Moon and Earth disks illuminated by the Sun. The results of this work were used in analysis of data of the Earth's atmosphere investigations with the AS "Astron." Detailed consideration of the telescope PSF allowed us to eliminate possible influence of the light scattered in the telescope on the results of remote sensing of the atmosphere. The scattered light causes a complicated non-monotonic time dependence of the photomultiplier signals in the spectrometer channels as the viewing beam removes from the Earth's disk edge illuminated by the Sun. This introduces essential distortions into the data of remote sensing of the terrestrial environment obtained by optical methods.[7]

It is an essential point that the experimental determination of PSF gave us an opportunity to make detailed calculations of the smoothing effects for the altitude dependence of the atmospheric spectral brightness observed in the Earth's limb under slant sensing of the atmosphere in the ultraviolet region from onboard the AS.[8] As to the use of the PSF the main result may be the conclusion that after launching space vehicles like Space Shuttle[9] there appears a thin layer of anthropogenic aerosol at the altitude about 100 km. This conclusion has been drawn from the direct comparison between the line diffusion function calculated from the PSF with the spectral brightness curve observed from the aerosol layer.

Experiments on investigating light scattering from the Earth's disk illuminated by the Sun have been carried out on July 9, 1983, when the apparatus traveled from the ascending orbit node to the apogee and on July 12, 1983, during its travel from the apogee to the descending node. The active mode of apparatus orientation has been used in these experiments. First, a

0235-6880/98/08 744-06 $02.00

segment sensor of the solar device has captured the Sun. As a result, one axis of the apparatus was fixed in the space. Then the apparatus has been rotated around the direction towards the Sun with the rotation period of 705 s using low thrust jets. After this, a momentum causing the rotation axis precession was applied to the apparatus. Due to the rotation about the axis and slow angular displacement of the apparatus rotation axis, scanning with the telescope 12″ field of view over a spatial region investigated was realized. "ased on ballistic and apparatus orientation data, the data of observations (the photomultiplier read-outs) were then referred to the coordinate system rigidly bound to the apparatus.

Two-dimensional distribution of relative signal intensity I/I_0, where I_0 is the mean signal intensity when observing the illuminated Earth's disk, obtained on July 9, 1983 is presented in Fig. 1. Here, the angular coordinates θ and φ are the coordinates of the center of the Earth's disk observed relative to the apparatus coordinate system. The $\{\mathbf{e}_\theta, \mathbf{e}_\varphi, \mathbf{e}_\gamma\}$ axes orientation of this system relative to the obliquely cut blind of the telescope is schematically shown at the upper right corner of the figure. The unit vector $\mathbf{e}_\gamma$ is directed along the telescope optical axis, i.e., along its viewing beam. The angular coordinates θ and φ correspond to transition into the spherical coordinate system with the poles on the $\mathbf{e}_\gamma$ axis. Here, θ is the latitudinal angle and φ is the azimuth angle measured from the $\mathbf{e}_\gamma$ axis. Figure 1 also presents the Earth's disk observed. Its angular diameter is 4.2°. Isolines are symmetric for $\theta < 0$ and $\theta > 0$; therefore they are not shown in the figure. The experiment lasted 2 hours and 30 minutes. Thirteen full revolutions about the direction towards the Sun were made during this time. The scanning has been performed with the step of 0.2° in θ and approximately 1° displacement in φ for two successive scans. Approximately 10^3 read-outs were taken, for which the signal intensity exceeded the background level. The mean distance to the Earth was 177 thousand kilometers. The initial signal was preliminary reduced by the background level that was equal to 66 pulses/s. The boundary isoline *1* presented in the figure corresponds to the signal-to-noise ratio equal to unity. The signal intensity distribution obtained on July 12, 1983, from the distance of 107 km from the Earth is similar to that shown in Fig. 1, but the angular size of the Earth's disk is here 6.8°.

Symmetry of the distribution observed is related with the telescope design symmetry, including the design of the spectrometer entrance slit, about the $\theta = 0$ plane, as well as with the peculiar orientation of the apparatus relative to the Sun. It is important to note that spatial pattern of the signal intensity shown in Fig. 1 is actually symmetric about the "Sun – Earth center – apparatus" plane, whereas the angles between this plane and the ecliptic and equator planes were equal to 51 and 60.5°, respectively.

Signal intensity $I(\Omega')$ may be related to the source brightness distribution $B(\theta, \varphi)$, if we introduce an instrumental function (effective point spread function) $A(\theta, \varphi)$ in the following way:

$$I(\Omega') = k \int_{\Omega'} B(\theta, \varphi)\, A(\theta, \varphi)\, d\Omega, \qquad (1)$$

where k is the scaling coefficient; θ and φ are radiation source coordinates in the apparatus coordinate system; Ω' is the radiation source area over which integration is being carried out; $d\Omega = \cos\theta\, d\theta\, d\varphi$; $\theta, \varphi \in \Omega'$. $I(\Omega')$ expresses the functional dependence of the signal intensity on the position of an extended radiation source.

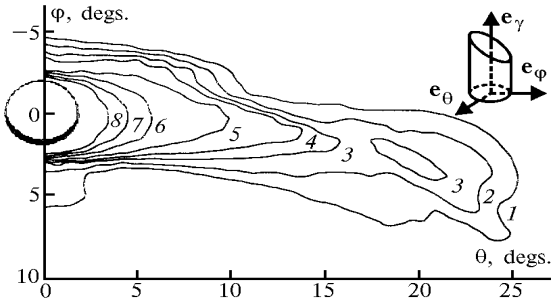

FIG. 1. Two-dimensional distribution of signal intensity I/I_0 when observing the Earth's disk illuminated by the Sun from onboard the AS "Astron." Figures denote the isolines I/I_0: $1.7\cdot10^{-6}$ (1), $4.6\cdot10^{-6}$ (2), $1.1\cdot10^{-5}$ (3), $1.9\cdot10^{-5}$ (4), $4.2\cdot10^{-5}$ (5), $1.3\cdot10^{-4}$ (6), $2.1\cdot10^{-4}$ (7), and $4.2\cdot10^{-4}$ (8). The line near the boundary of the illuminated part of the Earth's disk corresponds to $1.6\cdot10^{-3}$.

We can simplify Eq. (1), by replacing the local source brightness $B(\theta, \varphi)$ for its mean value B_0 and choosing the normalizing condition for $A(\theta, \varphi)$ as follows:

$$\int_{4\pi} A(\theta, \varphi)\, d\Omega = 1. \qquad (2)$$

Since the points from the vicinity of the 12″ field of view significantly contribute to the integral in Eq. (2) we can, according to Eq. (1), quite accurately assume that $kB_0 = I_0$, where I_0 is the mean signal intensity recorded in direct observation of the points at the radiation source, e.g., illuminated part of the Earth's disk. So, we can write Eq. (1) in the form

$$\frac{I(\Omega')}{I_0} = \int_{\Omega'} A(\theta, \varphi)\, d\Omega. \qquad (3)$$

The telescope point spread function[1] $a(\theta, \varphi \mid \theta'', \varphi'')$ characterizes, by definition, the radiation density at the point (θ'', φ'') in the telescope focal plane as a response to the effect of the point radiation source with the coordinates (θ, φ). Experimental determination of the PSF can be reduced to measurement of the radiation flux ΔW incident on the preset area ΔS in the telescope focal plane. Finite value of ΔS governs the corresponding

scale for the PSF averaging. In this case, $A(\theta, \varphi)$ characterizes the radiation flux having passed through the spectrometer input aperture of 12 seconds of arc having the area of 0.16 mm^2. Theoretically the PSF is determined through the radiation incident on the surface element ΔS from the upper hemisphere within 2π sr solid angle. Experimentally, there are always some limitations on the angle of incidence. In our case, these limitations are associated with the spectrometer light-gathering power. The function $A(\theta, \varphi)$ characterizes the radiation flux coming within the spectrometer input aperture. This radiation is reflected by the spectrometer grating; and it contributes to the signal, in particular, in the zeroth order of the spectrum. Since relative apertures of both the receiving optics and of the grating are matched (1:10), $A(\theta, \varphi)$ function, for radiation sources that are observed within 12″-aperture field of view or near it, practically corresponds to the total radiation flux incident on ΔS from a point source within the upper hemisphere. At source displacement off the aperture optical axis by at least more than 1′, $A(\theta, \varphi)$ and $a(\theta, \varphi \mid 0, 0)$ should be proportional to each other.

We have reconstructed the values of unknown two-dimensional function $A(\theta, \varphi)$ by solving the integral equation (3) with the use of the two-dimensional data array presented in Fig. 1. The results are shown in Fig. 2. For the convenience of the data presentation on the logarithmic scale, the function values near zero were replaced by 10^{-4}. Nonzero function values vary from 10^{-4} to 5. In view of the fact that this problem is ill-posed, the solution of the integral equation (3) has been obtained within the framework of the Tikhonov regularization method.[10] The well-known Tikhonov stabilizer of the second order has been used. The values of $A(\theta, \varphi)$ have been calculated at nodes of a two-dimensional grid specified in the region $0 < \theta < 28°$, $-7° < \varphi < 9°$ ($0.3° < r < 28°$, $r = \sqrt{\theta^2 + \varphi^2}$). Outside this region, $A(\theta, \varphi) = 0$. The problem symmetry has been taken into account by the condition that $A(\theta, \varphi) = A(-\theta, \varphi)$. When making up the functional, we have used the weighting factors proportional to (I/I_0). The regularization parameter has been fit to the experimental data error based on the discrepancy criterion. The relative error of I/I_0 determination was from 3 to 10%.

According to the estimations made, the main contribution to the error came from the uncertainty in assignment of the observation coordinates. The error of photon counting was also considered. When calculating the integrals, we considered the exact shape of the visible illuminated Earth disk (see Fig. 1). The error of calculating the integral did not exceed 2%. In general, the function $A(\theta, \varphi)$ has a peculiarity, namely, its values sharply increase as r tends to zero. "ecause of this fact as well as due to limited computer capabilities, we have used grids with different steps in different regions. In the case of $r < 2.5°$, the grid step was equal to the scan step $\Delta\theta = \Delta\varphi = 0.2°$, whereas at $r > 2.5°$ it was possible to use a grid with the step of 1°. As a result, a good agreement is observed between the experimental dependence of the signal intensity I/I_0 and that calculated from the reconstructed instrumental function $A(\theta, \varphi)$. It should be noted that temporal dependence of the signal intensity has a complicated and nonmonotonic behavior at recording of a scattered light.[7]

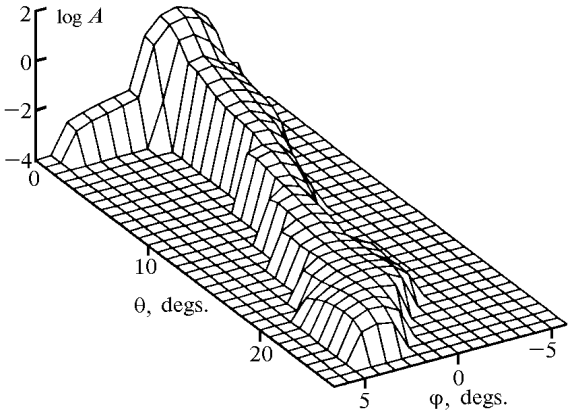

FIG. 2. Effective point-spread function for AS "Astron" telescope at $0.3° < r < 26°$ *obtained from the data of observation of the illuminated Earth's disk.*

Investigations of $A(\theta, \varphi)$ function behavior at $r < 0.3°$ were carried out based on the data obtained from scanning of the moon disk on July 15, 1983. During this experiment, telescope axes were fixed relative to stars, while the apparatus was passing the orbit apogee being comparatively slow moving. Movement of the telescope line of sight on the moon disk was by 90% caused by the moon movement along its orbit about the Earth. The moon velocity vector therewith was almost perpendicular to the sight line, the angle between them was 73.6°. The distance from the apparatus was 207 thousand kilometers to the Earth and 516 thousand kilometers to the moon. The trajectory of the viewing beam on the moon disk is schematically shown in Fig. 3. The moon phase visible from the apparatus was 3/4. The moon angle diameter was 0.38°. The trajectory practically coincided with the horizontal symmetry line that bisects the disk. The angle between the trajectory and the symmetry line was approximately 2°. The trajectory intersected the moon terminator line to the south of the Sultriness " ay of the Island Sea.

The experimental dependence of the signal intensity I/I_0 on the distance α, in units of arc, between the telescope viewing beam and the point where the trajectory intersects the moon terminator is presented in Fig. 3. The intensity leap in the curve points to the passage of the telescope field of view through the terminator. The signal intensity averaged over the curve part (see Fig. 3) corresponding to the illuminated moon surface was taken as I_0. Since, according to Eq. (1), the signal I is determined by the local brightness, this favors the normalizing condition (3) to hold, when reconstructing function A from Eq. (2). The averaged value indicated is 1.5 times less than the average value for all trajectory points corresponding to the illuminated moon part. Read-outs were taken every 4.9 s, the angle step was 2.2 min. of arc or 5.5 km on the moon disk. The total number of points on the curve (Fig. 3) is about 1300. Background

values were subtracted from the experimental intensity values. An ash light contribution to I/I_0 was less than 10^{-4} and it was at least an order of magnitude lower than the signal value, when moving along the dark side of the moon ($0.1° < \alpha < 0$).

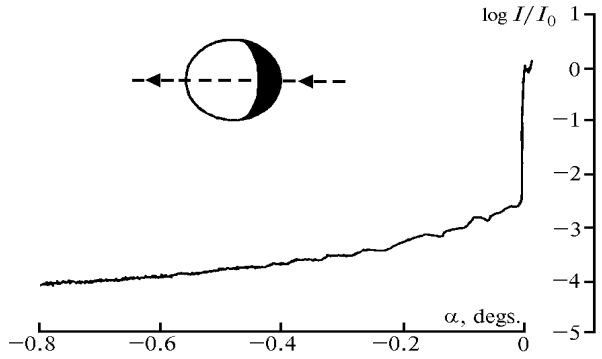

FIG. 3. Results of observation from the AS "Astron" of the moon disk illuminated by the Sun .

In the coordinate system rigidly bounded to the apparatus and determined in the same way as in the studies of illuminated Earth's disk (see Fig. 1), the trajectory of the viewing beam correlates with the motion of the visible moon disk center along φ axis at $\theta \approx 0$. As reconstruction of the two-dimensional function $A(\theta, \varphi)$ is impossible in full measure, we took that $A(\theta, \varphi)$ depends only on distance r from the field of view center $(\theta, \varphi) = 0$, i.e. $A(\theta, \varphi) = A(r)$. It was possible to introduce two functions for each r: $A_+(r)$ defined for $\varphi > 0$ and $A_-(r)$ defined for $\varphi < 0$. These two functions can be replaced by one $A(\varphi)$: $A(\varphi)$ is equal to $A_+(r)$ at $\varphi > 0$ and $A_-(r)$ at $\varphi < 0$. To reconstruct $A(\varphi)$, we used the algorithm with a regularization by Tikhonov method.

The results of $A(\varphi)$ reconstruction from the experimental dependence I/I_0 (see Fig. 3) for $-0.8° < \varphi < 40''$ are presented in Fig. 4. The curve *1* is a direct estimation of $A(\varphi)$, according to Eq. (3), for $-0.8° < \varphi < 0.64°$. "y virtue of comparatively slow change of the function and small angular size of the moon disk, the estimation has been made using the approximate relationship

$$I/I_0 = A\Delta\Omega_L ,$$

where $\Delta\Omega_L$ is the area of the illuminated part of the moon disk, in units of arc, with regard for the position of the center of gravity of the illuminated part of the disk. At $0.6° < \varphi < +10''$, the integral equation (3) has been solved using Tihkonov's regularization method (curve *2*). In the vicinity of $\varphi = 0$, where the problem of instrumental function reconstruction in the 12″-aperture field of view has actually been solved, we used a grid with the minimum step of 2 seconds of arc. Whereas in the other parts of the region, the results depended only weakly on the grid step $\Delta\varphi$ as it changed from 2 to 44 seconds of arc. Curve *3* shows, for a comparison, the function values reconstructed from data of the Earth's disk observation.

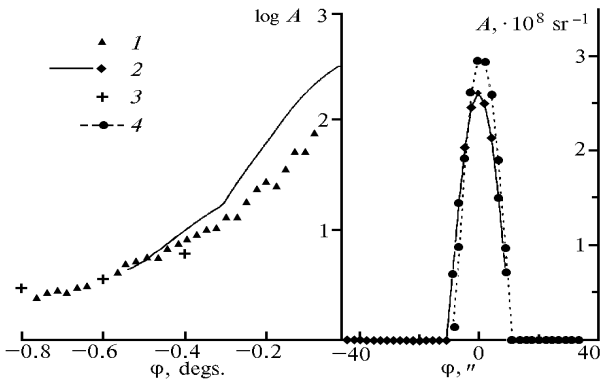

FIG. 4. Effective point spread function for the AS "Astron" telescope at $0° < r < 0.8°$ obtained from the data of illuminated moon disk observations: simple estimation according to Eq. (3) – (1), reconstruction from the data shown in Fig. 3 (2), reconstruction from the data of illuminated Earth's disk observations (3), reconstruction from the data of displacement from the illuminated edge of the moon disk (4).

As one can see, the results are in a rather good agreement. At the same time, one should pay proper attention to the fact that such an agreement was obtained for curves *1* and *2* with the difference in the grid steps of approximately two orders of magnitude and additional assumptions on the $A(\theta, \varphi)$ function peculiarities introduced when calculating the *1* curve. The dependence I/I_0 calculated from reconstructed $A(\theta, \varphi)$ values is close to the experimental one, while being smoother. Curve *4* presents the results of $A(\theta, \varphi)$ function reconstruction from I/I_0 dependence obtained under displacement of the telescope sight line off the illuminated moon disk. "ecause in this case the I/I_0 dependence has been obtained only for small distance from the moon edge, the reconstruction of $A(\theta, \varphi)$ was possible only for small values of φ. The absence of distinct peak broadening at $\varphi = 0$ (curve *2*, right-hand part of Fig. 4) as compared to the peak on the curve *4* is an *a posteriori* proof that, in the passage across the terminator, a narrow light–shadow border was actually observed. At a displacement off from the moon edge, the condition of the sharp light–shadow border was kept true (2″ corresponds to 5 km on a linear scale).

The maximum value of the instrumental function, A_{max}, at the center of the 12″-aperture field of view at $\varphi = 0$ equals approximately to $3 \cdot 10^8$ sr^{-1}. This value well agrees with the value $A_{max} = 4 \cdot 10^8$ obtained from the geometrical considerations: $A_{max} \cdot \Delta\Omega_0 \approx 1$, where $\Delta\Omega_0$ is the area of the 12″-aperture in units of arc. The peak half-width is $\Delta\varphi_{0.5} \approx 12–13''$ and $\Delta\varphi_{0.1} \approx 16''$. At $r > 20''$, the instrumental function $A(\theta, \varphi)$ changes

slightly at the 12″-scale and, with regard to the incident angle restrictions, becomes proportional to the usual point spread function $a(\theta, \varphi \mid 0, 0)$. Therefore, we can consider $A(\theta, \varphi)$ as an effective point spread function. And the value of $A(\theta, \varphi)$ becomes being only caused by the contribution from parasitic light scattered in the telescope.

As one can see from the Fig. 4, at $\varphi < -20''$ outside the field of view of the 12″ aperture, it is possible to isolate the region $-0.3° < \varphi < -20''$, where the rate of the function $(d \ln A/d\varphi)$ change is higher than it is at $\varphi < -0.3°$. Physically this region is associated with the fact that inside it the initial beam has to be focused at the spectrometer entrance slit. This entrance slit is made of polished steel as a tetrahedral pyramid having round holes serving as spectrometer input apertures. At $\varphi < 0.3°$ ($r > 0.3°$), the function behavior is governed by other physical factors.

As seen from Fig. 2, from the plot of the two-dimensional function $A(\theta, \varphi)$, one can isolate the region $0.3° < r < 2°$, where the function is bell-shaped and its values differ essentially from those beyond this region at $r > 2°$. The $A(\theta, \varphi)$ behavior in the region indicated is physically determined by the fact, that at such angles the initial beam from the point source reflected from the primary and secondary mirrors passes through the central hole in the primary mirror. At larger r values, the optical system makes a blurred source image on the primary mirror surface. As seen from the Fig. 2, the function $A(\theta, \varphi)$ has the general view of an unequilateral cross at $r > 2°$. With the $A(\theta, \varphi)$ reconstruction accuracy up to the level of 10^{-4}, the longest arms expand along θ axis to $\pm 26°$, whereas along φ axis one of them expands to $\varphi = +6°$ and another one expands to $\varphi = -5°$.

Different ranges of variation of the effective point spread function $A(\theta, \varphi)$ argument give different contributions to the total signal intensity. These contributions, in accordance with Eq. (3), can be characterized by values of $(I/I_0)_i = \int A \, d\Omega_i$, where integration is carried out within the corresponding ranges Ω_i of the argument variation. Thus, for the range $r < 20''$ including the 12″-aperture field of view, $(I/I_0)_1 \approx 1$; for $20'' < r < 0.3°$ corresponding to the spectrometer entrance slit, $(I/I_0)_2 \approx 6.6 \cdot 10^{-3}$; for $0.3° < r < 20$, when the initial beam from a point source passes through the central hole in the primary mirror, $(I/I_0)_3 \approx 2.4 \cdot 10^{-3}$; for $2° < r < 31°$ $(I/I_0)_4 \approx 0.5 \cdot 10^{-3}$. In accordance with these results, when displacing the telescope field of view off from the illuminated moon disk at a distance from 20″ to several minutes of arc, the signal intensity I/I_0 caused by the scattered light should be approximately $(I/I_0)_2/2 \approx 3.3 \cdot 10^{-3}$ (with regard for small angular size of the moon equal to 0.38°).

According to Fig. 3, when crossing the moon terminator, a sharp decrease is observed in the signal intensity I/I_0 from 1 to $3 \cdot 10^{-3}$ that well agrees with this value. The same result has been obtained when displacing off from the edge of the illuminated moon disk. When displacing the telescope field of view from the Earth's edge, the scattered light intensity should be a bit less than $[(I/I_0)_2 + (I/I_0)_3 + (I/I_0)_4]/2 = 4.7 \cdot 10^{-3}$. However, in Fig. 1, the boundary isoline of the signal intensity passing along the edge of the illuminated part of the Earth's disk corresponds to $I/I_0 = 1.6 \cdot 10^{-3}$. This was done to eliminate the data for $r < 0.3°$ from the data array at large scanning step of 0.2°. At the same time, it should be mentioned that in the experiments on tangent Earth atmosphere sensing[7,8] at a scanning step less than 1″ and when leaving the atmospheric limb, the signal intensity I/I_0 in the zeroth order of the spectrum was approximately equal to $4 \cdot 10^{-3}$.

In conclusion, we should like to note the following. The variation range of the reconstructed instrumental function values (the effective point spread function), equal approximately to 10^{13}, results from a large variation range (10^7 times) of the areas of the function characteristic regions ($r < 10''$ and $r < 10°$) at the dynamic range of radiation flux recording being on the order of 10^6.

REFERENCES

1. A.N. Valentyuk and K.G. Prokhod'ko, *Optical Image in Remote Observation* (Nauka i tekhnika, Minsk, 1991), 359 pp.
2. V.B. Veterell, in: *Space Optics* (Mashinostroenie, Moscow, 1990), pp. 43–72.
3. G.F. Bennet, Yu.L. Stendford, and Yu.M. Bennet, in: *Space Optics* (Mashinostroenie, Moscow, 1990), pp. 461–475.
4. A.A. Boyarchuk, R.E. Gershberg, L.V. Granitskii, et al., Pis'ma v Astrofiz. Zh. **10**, No. 3, 163–174 (1984).
5. A.A. Boyarchuk, Itogi Nauki i Tekhniki, VINITI, "Astronomiya" **31**, 198–212 (1986).
6. G.M. Popov, *Modern Astronomy Science* (Nauka, Moscow, 1988), 192 pp.
7. L.V. Granitskii and A.A. Cheremisin, in: *Abstracts of Papers at the All-Union Conference on Geophysical Phenomena in the Auroral Zone* (SibIZMIR, Irkutsk, 1988), p. 11.
8. A.A. Cheremisin, L.V. Granitskii, V.M. Myasnikov, N.V. Vetchinkin, and V.V. Slabko, Atmos. Oceanic Opt. **10**, No. 12, 891–895 (1997).
9. A.A. Cheremisin, L.V. Granitskii, V.M. Myasnikov, and N.V. Vetchinkin, Atmos. Oceanic Opt. **10**, No. 12, 885–890 (1997).
10. A.N. Tikhonov, A.V. Goncharovskii, V.V. Stepanov, and A.G. Yagola, *Numerical Methods for Solution of Ill-Posed Problems* (Nauka, Moscow, 1990), 232 pp.